J Ind Microbiol Biotechnol (2015) 42:671–680
DOI 10.1007/s10295-015-1604-y

BIOCATALYSIS

SIMB
Society for Industrial Microbiology and Biotechnology

Expression of a novel epoxide hydrolase of *Aspergillus usamii* E001 in *Escherichia coli* and its performance in resolution of racemic styrene oxide

Die Hu · Cun-Duo Tang · Biao Yang · Jia-Chi Liu · Tao Yu · Chao Deng · Min-Chen Wu

Received: 4 September 2014 / Accepted: 16 February 2015 / Published online: 3 March 2015

Abstract The full-length cDNA sequence of *Aueh2*, a gene encoding an epoxide hydrolase of *Aspergillus usamii* E001 (abbreviated to AuEH2), was amplified from the total RNA. Synchronously, the complete DNA sequence containing 5′, 3′ flanking regions, eight exons and seven introns was cloned from the genomic DNA. In addition, a cDNA fragment of *Aueh2* encoding a 395-aa AuEH2 was expressed in *Escherichia coli*. The catalytic activity of recombinant AuEH2 (re-AuEH2) was 1.44 U/ml using racemic styrene oxide (SO) as the substrate. The purified re-AuEH2 displayed the maximum activity at pH 7.0 and 35 °C. It was highly stable at a pH range of 5.0–7.5, and at 40 °C or below. Its activity was not obviously influenced by β-mercaptoethanol, EDTA and most of metal ions tested, but was inhibited by Hg^{2+}, Sn^{2+}, Cu^{2+}, Fe^{3+} and Zn^{2+}. The K_m and V_{max} of re-AuEH2 were 5.90 mM and 20.1 U/mg towards (*R*)-SO, while 7.66 mM and 3.19 U/mg towards (*S*)-SO. Its enantiomeric ratio (*E*) for resolution of racemic SO was 24.2 at 10 °C. The experimental result of re-AuEH2 biasing towards (*R*)-SO was consistent with the analytical one by molecular docking (MD) simulation.

Keywords *Aspergillus usamii* · Epoxide hydrolase · Styrene oxide · Enantioselectivity · Molecular docking simulation

D. Hu and C.-D. Tang contributed equally to this work.

Electronic supplementary material The online version of this article (doi:10.1007/s10295-015-1604-y) contains supplementary material, which is available to authorized users.

D. Hu
Key Laboratory of Carbohydrate Chemistry and Biotechnology, School of Biotechnology, Ministry of Education, Jiangnan University, 1800 Lihu Road, Wuxi 214122, Jiangsu, People's Republic of China

C.-D. Tang
China-UK-NYNU-RRes Joint Laboratory of Insect Biology, Nanyang Normal University, 1638 Wolong Road, Nanyang 473061, Henan, People's Republic of China

B. Yang · J.-C. Liu · C. Deng · M.-C. Wu (✉)
Wuxi Medical School, Jiangnan University, 1800 Lihu Road, Wuxi 214122, Jiangsu, People's Republic of China
e-mail: biowmc@126.com

T. Yu
School of Pharmaceutical Science, Jiangnan University, 1800 Lihu Road, Wuxi 214122, Jiangsu, People's Republic of China

Introduction

Epoxide hydrolases (EHs, EC 3.3.2.3), existing widely in microorganisms, plants, invertebrates and mammals, catalyze the hydrolysis of epoxides to the corresponding vicinal diols. EHs are cofactor-independent enzymes, which are active in the absence of coenzymes or prosthetic groups [21]. Some EH-encoding genes have been cloned, characterized and expressed in heterologous cells. Compared to EHs from other organisms, microbial ones attracted more attention owing to their superior properties such as broad substrate specificity and high enantioselectivity [12]. To date, almost all known EHs have been classified into a large superfamily sharing a common core topology of the three-dimensional (3-D) structure, known as α/β hydrolase fold, whereas their primary structure identities are low [4]. EHs have an absolutely conserved catalytic triad Asp-Glu/Asp-His. Asp acts as a nucleophile, which attacks the oxirane ring carbon forming a substrate-enzyme intermediate. Subsequently, the intermediate at the enzymatic active center is hydrolyzed by a water molecule activated by general-base

His and charge-relay Glu/Asp. In addition, two Tyr residues providing hydrogen bonding to the epoxide oxygen are also conserved in EHs [28].

Resolution of racemic epoxides by enantioselective EHs can generate enantiopure epoxides and vicinal diols, which are versatile synthons for the preparation of highly value-added bioactive compounds such as pharmaceuticals, agrochemicals and fine chemicals [20]. Related to racemic epoxide, the theoretical yield of enantiopure epoxide is 50 %, while the yield of chiral vicinal diol could reach 100 % in some specific cases [21]. In contrast to chemical synthesis of enantiopure epoxides and/or diols, biotransformation by EHs, an environmentally friendly process without needs of heavy metal-based catalysts, possessed higher enantiomeric excess (ee) and yield [8]. Recently, several enantioselective EHs have been applied to the resolution of racemic styrene oxide (SO) to produce (*S*)-SO, an important drug intermediate for the synthesis of nematocide, anticancer agent—levamisole, and anti-HIV agent—(−)-hyperolactone C [23].

Some microbial EHs have been isolated and characterized, but their industrial production and application were hindered by the low catalytic activity and/or enantiomeric ratio (*E*). Therefore, more interests are being focused on the gene cloning and expression of novel EHs with superior properties, and on the improvement of existing EHs by genetic engineering. In this work, we reported the cloning and bioinformatics analysis of both the full-length cDNA and complete DNA sequences of *Aueh2* from *A. usamii* E001. In addition, an AuEH2-encoding cDNA fragment was heterologously expressed in *E. coli* BL21(DE3). The expressed re-AuEH2 was purified to homogeneity, characterized and applied to the resolution of racemic SO to obtain (*S*)-SO. The enantioselective mechanism of re-AuEH2 biasing towards (*R*)-SO was analyzed by MD simulation of AuEH2 with (*R*)-SO or (*S*)-SO.

Materials and methods

Strains, plasmids, and culture media

Aspergillus usamii E001, isolated from the soil in China and preserved in our laboratory [24], was used for total RNA and genomic DNA extraction. The strain was cultured at 30 °C in a medium containing (w/v): 1 % tryptone, 0.5 % yeast extract, 2 % glucose, 0.5 % $(NH_4)_2SO_4$ and 0.1 % racemic SO (TCI, Tokyo, Japan), pH 6.0. *Escherichia coli* JM109 and plasmid pUCm-T (Sangon, Shanghai, China) were used for gene cloning and DNA sequencing, while *E. coli* BL21(DE3) and pET-28a(+) (Novagen, Madison, WI, USA) for gene expression. *E. coli* JM109 and BL21(DE3) were cultured at 37 °C in a Luria–Bertani medium comprising (w/v): 1 % tryptone, 0.5 % yeast extract and 1 % NaCl, pH 7.2.

Cloning of the full-length cDNA sequence of *Aueh2*

First, the 3′-end cDNA fragment was amplified using the RNA PCR Kit (TaKaRa, Dalian, China). In brief, the first-strand cDNA was reversely transcribed from *A. usamii* total RNA with a primer dT-MP. Using the resultant first-strand cDNA as the template, the first-round PCR was carried out with EH-F1 and MP under the following conditions: 30 cycles of at 94 °C for 30 s, 51 °C for 30 s and 72 °C for 50 s. PCR products were gel-purified, and then subjected to the second-round PCR with EH-F2 and MP for confirmation (nested PCR). Next, the 5′-end cDNA fragment, originating from the starting point of transcription, was amplified using the 5′-Full RACE Kit (TaKaRa, China). The first-strand cDNA was used as the template for the first-round PCR with OP and EH-R2, and subjected to the second-round PCR with IP and EH-R1 for confirmation. All PCR primers (except those provided by Kits) were synthesized by Sangon (Shanghai, China) as listed in Table S1. Finally, the full-length cDNA sequence of *Aueh2* was obtained by overlapping the amplified 5′- and 3′-end cDNA fragments.

Cloning of the complete DNA sequence of *Aueh2*

First, the central DNA fragment was directly amplified from the genomic DNA extracted from *A. usamii* as reported previously [24], by conventional PCR with EH-F and EH-R. Next, the 5′ or 3′ flanking DNA fragment was amplified by T-hairpin structure-mediated PCR (abbreviated to THSM-PCR) as described below. Finally, the complete DNA sequence of *Aueh2* was obtained by assembling the amplified 5′, 3′ flanking and central DNA fragments.

THSM-PCR, a novel technique developed in our laboratory to amplify the 5′ or 3′ flanking region of a known DNA fragment, was conducted by five steps (Fig. S1). First, the *A. usamii* genomic DNA was digested with *Xba* I, which was screened through a series of pre-experiments. Second, the cohesive ends of digested DNA fragments were filled in and added an adenine nucleotide (A) at 3′-ends with *rTaq* DNA polymerase at 72 °C for 10 min. Third, a T-hairpin structure used as the adapter was formed by treating a specifically designed oligonucleotide under the following conditions: a denaturation at 94 °C for 3 min, followed by annealing to 25 °C at a rate of 1 °C/s and lasting for 30 min. The fourth step was to ligate the second step's products with adapter at 16 °C for 8 h. Finally, the ligated DNA samples were amplified with HSO-F and EH-R to obtain the 5′ flanking DNA fragment, and subjected to the second-round PCR with HSO-F and EH-R3 for confirmation. Similarly,

the 3′ flanking DNA fragment was amplified by the first-round PCR with HSO-F and EH-F, and confirmed by the second-round PCR with HSO-F and EH-F3. A T-hairpin structure oligonucleotide (HSO-T) and PCR primers were listed in Table S1.

Bioinformatics analysis of the amino acid and nucleotide sequences

The homology sequence search at NCBI website (http://www.ncbi.nlm.nih.gov/) was performed using the BLAST server, while the multiple alignment of amino acid sequences among fungal EHs using the ClustalW2 program (http://www.ebi.ac.uk/Tools/msa/Clustalw2). The prediction of a promoter region of *Aueh2* and its characterization were carried out using the TFSEARCH (http://www.cbrc.jp/research/db/TFSEARCH.html), together with the PLACE (http://www.dna.affrc.go.jp/PLACE/signalscan.html), while the localization of exon/intron boundaries using the GeneMark (http://opal.biology.gatech.edu/GeneMark/eukhmm.cgi). The AuEH2-encoding cDNA fragment of *Aueh2*, that is, an open reading frame (ORF), was predicted by NCBI ORF Finder (http://www.ncbi.nlm.nih.gov/gorf/gorf.html). The physicochemical properties of AuEH2 were identified using the Protparam program (http://au.expasy.org/tools/protparam.html).

Enzyme activity and protein assays

EH activity was measured as described previously [26] with slight modification. In brief, 0.1 ml of suitably diluted EH solution was mixed with 0.9 ml of 10 mM racemic SO in 50 mM K_2HPO_4–KH_2PO_4 buffer (pH 7.0). After incubation at 37 °C for 15 min, the reaction was terminated by adding 3 ml of methanol. The generated phenyl glycol was analyzed by high-performance liquid chromatography (HPLC) using an UltiMate-3000 system (Dionex, Sunnyvale, CA, USA) equipped with a C18 reverse-phase column (Chrom-Matrix, Wuxi, China; 4.6 × 260 mm). The mobile phase of methanol/H_2O (75:25, v/v) was used at a flow rate of 0.8 ml/min, and monitored at 220 nm with a VWD-3100 detector (Dionex, USA). One unit (U) of EH activity was defined as the amount of enzyme generating 1 μmol of phenyl glycol per min under the above assay conditions.

Sodium dodecyl sulfate–polyacrylamide gel electrophoresis (SDS-PAGE) was performed using the method of Laemmli [10]. The separated proteins were visualized by staining with Coomassie Brilliant Blue R-250 (Sigma, St. Louis, MO, USA), whose apparent molecular weights were estimated using a Quantity One software based on the standard marker proteins. The protein concentration was measured with the BCA-200 Protein Assay Kit (Pierce, Rockford, IL, USA) using bovine serum albumin as the standard.

Construction and expression of the recombinant *E. coli*

With the information of the cloned full-length cDNA sequence of *Aueh2*, EH-F and EH-R (Table S1) were designed and used to amplify the AuEH2-encoding cDNA fragment from the first-strand cDNA reversely transcribed from *A. usamii* total RNA. Conditions for PCR amplification were 30 cycles of at 94 °C for 30 s, 55 °C for 30 s and 72 °C for 75 s. The target PCR product was gel-purified, digested with *Eco*R I and *Not* I, and inserted into pET-28a(+) digested with the same enzymes. The resultant recombinant expression plasmid, pET-28a(+)-*Aueh2*, was transformed into *E. coli* BL21(DE3) forming a recombinant *E. coli*, designated *E. coli*/pET-28a-*Aueh2*. *E. coli* BL21(DE3) transformed with pET-28a(+) was used as the negative control (*E. coli* BLC). Expression of an AuEH2-encoding cDNA fragment in *E. coli* was performed as reported previously [27] with slight modification.

Purification of the expressed re-AuEH2

E. coli/pET-28a-*Aueh2* cells, induced by adding 0.2 mM IPTG at 28 °C for 8 h, were collected from 100 ml of cultured broth, and suspended in 10 ml of 20 mM Tris–HCl buffer (pH 7.9) containing 500 mM NaCl. After the cells were treated by ultrasonic, the resultant supernatant was loaded onto a nickel–nitrilotriacetic acid (Ni–NTA) column (Tiandz, Beijing, China; 1 × 6 cm) preequilibrated with a binding buffer (20 mM Tris–HCl, 500 mM NaCl, 20 mM imidazole, pH 7.9), followed by elution at a flow rate of 0.3 ml/min with the elution buffer that was the same as binding buffer except 200 mM imidazole. The eluent containing re-AuEH2 was dialyzed against 20 mM K_2HPO_4–KH_2PO_4 buffer (pH 7.0). All purification steps were performed at 4 °C unless stated otherwise.

Enzymatic properties of the purified re-AuEH2

The pH optimum of re-AuEH2 was measured under the standard assay conditions, except for 10 mM racemic SO in 50 mM Na_2HPO_4–citric acid buffer (pH 5.5–7.5) and Tris–HCl buffer (pH 7.5–9.0). To estimate its pH stability, aliquots of re-AuEH2 were incubated at 30 °C for 1 h at different pH values (Na_2HPO_4–citric acid buffer: pH 3.5–7.5, Tris–HCl buffer: pH 7.5–9.0 and NaOH–glycine buffer: pH 9.0–10.0). Its pH stability in this work was defined as a pH range, over which the residual re-AuEH2 activity retained over 85 % of its original activity. The temperature optimum of re-AuEH2 was assayed, at pH optimum, at temperatures ranging from 5 to 50 °C. For evaluating its thermostability, aliquots of re-AuEH2 were incubated at 40, 45 and 50 °C until 1 h. Here, its thermostability was defined as

a temperature, at or below which the residual re-AuEH2 activity was more than 85 % of its original activity.

For estimating the effects of β-mercaptoethanol, EDTA and an array of metal ions on its activity, aliquots of re-AuEH2 were incubated with additives at their final concentrations of 2 mM, respectively, in 20 mM K_2HPO_4–KH_2PO_4 buffer (pH 7.0) at 30 °C for 1 h. The enzyme without adding any additive was used as the control. The hydrolytic reaction rate (U/mg) of re-AuEH2 was measured under the standard assay conditions, except for (*R*)-SO or (*S*)-SO concentrations ranging from 2.5 to 20 mM. The K_m and V_{max} of re-AuEH2 were calculated by non-linear regression analysis using the Origin 9.0 software (http://www.originlab.com/). The catalytic constant k_{cat} was deduced using V_{max} and apparent molecular weight of re-AuEH2.

Resolution of racemic SO by re-AuEH2

Resolution of racemic SO was performed as follows: 0.1 mg of re-AuEH2 was mixed with 3 ml of 20 mM racemic SO in 50 mM K_2HPO_4–KH_2PO_4 buffer (pH 7.0), and followed by incubating at 10, 20 and 35 °C, respectively. Reaction samples (100 μl) were taken out at different periods, extracted with 400 μl ethyl acetate containing 1 mM n-pentanol (internal standard), and analyzed using

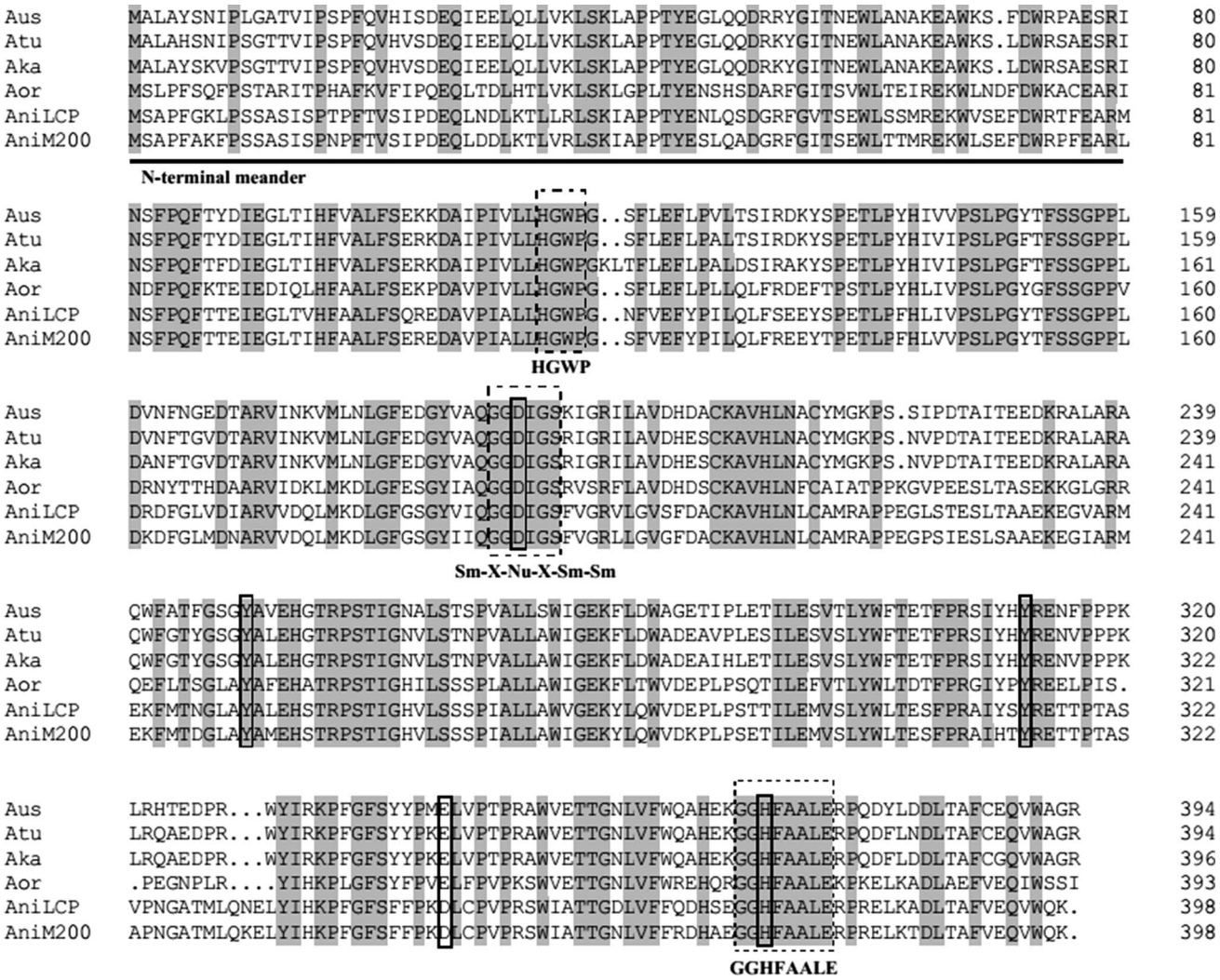

Fig. 1 The multiple alignment of primary structures among six fungal EHs using the ClustalW2 program. Aus, *A. usamii* (AGV05362, in this work); Atu, *A. tubingensi* (AGV76519); Aka, *A. kawachii* (GAA87738); Aor, *A. oryzae* (XP_001818311); AniLCP, *A. niger* LCP521 (CAB59813); and AniM200, *A. niger* M200 (ABF21120). The identical amino acid residues among six EHs are marked in *gray*. Several conserved motifs corresponding to the oxyanion hole of HGWP, nucleophile of GGDIGS and octapeptide of GGHFAALE are highlighted by *dashed box*. One catalytic triad (Asp191-His369-and Glu343) and two active site residues (Tyr249 and Tyr312) are shown in *boxes*. The 'N-terminal meander' of EHs is *underlined*

a GC-2014 apparatus (Shimadzu, Tokyo, Japan) equipped with a chiral CP-Chirasil-DEX CB column (Agilent, Santa Clara, CA, USA) and a flame ionization detector. The injector and detector were at 250 °C, and the column temperatures were programmed from 80 to 120 °C at a rate of 3 °C/min. The enantiomeric excess towards (*S*)-SO was calculated with an equation: ee = $[(S - R)/(S + R)] \times 100$ %, the yield of (*S*)-SO: yield = $[S/(S_0 + R_0)] \times 100$ %, and the enantiomeric ratio value: $E = [\ln (R/R_0)]/[\ln (S/S_0)]$. *R* and *S* are the final concentrations of (*R*)-SO and (S)-SO, respectively, while R_0 and S_0 the initial concentrations [3].

MD simulation between AuEH2 and (*R*)-SO or (*S*)-SO

Based on the known crystal structure of *A. niger* EH (AnEH, PDB: 1QO7) [28], the 3-D structure of AuEH2 was homologically modeled using the MODELLER 9.9 (http://salilab.org/modeller/). Synchronously, the 3-D structure of (*R*)- or (*S*)-SO was handled using a ChemDraw Ultra 12.0 software (www.cambridgesoft.com/). The interaction between 3-D structures of AuEH2 and (*R*)- or (*S*)-SO was predicted by MD simulation using the AutoDock 4.2 (http://autodock.scripps.edu) to locate the most suitable binding position and orientation. Then, the molecule-docked complex was optimized by GROMACS 4.5 (http://www.gromacs.org/). Based on the conformation of AuEH2 docking with (*R*)- or (*S*)-SO, the distance between O-atom of nucleophile Asp and unsubstituted C-atom of oxirane ring as well as the hydrogen bond length between hydroxyl group of Tyr and O-atom of oxirane ring was measured by PyMol (http://pymol.org/). The binding free energy (ΔG_{bind}) of a receptor (AuEH2 in this work) docking with a ligand [(*R*)- or (*S*)-SO], contrary to the affinity between them, was calculated using the molecular mechanics Poisson-Boltzmann surface area (MM-PBSA) method [13].

Results and discussion

Cloning and analysis of the full-length cDNA sequence

A 668-bp 3′-end cDNA fragment of *Aueh2* was cloned by 3′ RACE using the RNA PCR Kit, while a 1459-bp 5′-end cDNA fragment by 5′ RACE using the 5′-Full RACE Kit. The full-length cDNA sequence of 1559 bp in length was obtained by overlapping the cloned 3′- and 5′-end cDNA fragments. It contains a 273-bp 5′-untranslated region, a 1188-bp ORF encoding 395 amino acids, and a 98-bp 3′-untranslated region in which the AATAAA sequence used as the polyadenylation signal was recognized (Fig. S2). The cDNA sequence of *Aueh2* shared 65–98 % identities with those of other fungi EH genes.

Cloning and analysis of the complete DNA sequence

A 1485-bp central DNA fragment of *Aueh2* was firstly amplified from *A. usamii* genomic DNA by conventional PCR. Next, the 3′ and 5′ flanking DNA fragments of 826 and 544 bp in length were amplified, respectively, by THSM-PCR (Fig. S1). Finally, the complete DNA sequence of 2481 bp in length was obtained by assembling the amplified 3′ and 5′ flanking and central DNA fragments. Compared with the full-length cDNA, the complete DNA contains seven introns ranging from 46 to 63 bp. All exon/intron boundaries conform to the canonical GT-AG rule except the first and third one. A TATAAA sequence as a classical TATA box locates at 30 bp upstream the transcription starting point (A) as shown in Fig. S2. The DNA sequence of *Aueh2* along with its deduced amino acid sequence has been deposited in the GenBank database under the accession number KF061095.

Analysis of the primary structure of AuEH2

The primary structure of 395-aa AuEH2 was deduced from ORF of *Aueh2*. The theoretical molecular weight and isoelectric point of AuEH2 were predicted to be 44.6 kDa and 5.4, respectively, by Protparam program. The alignment of primary structures showed that the identities of AuEH2 with other 5 fungal EHs from *A. tubingensi* (AGV76519), *A. kawachii* (GAA87738), *A. oryzae* (XP_001818311), *A. niger* LCP (CAB59813) and *A. niger* M200 (ABF21120) were 91.1, 89.2, 58.2, 58.2 and 56.5 %, respectively. The multiple alignment among 6 fungal EHs displayed that AuEH2 has several conserved motifs identical to those of

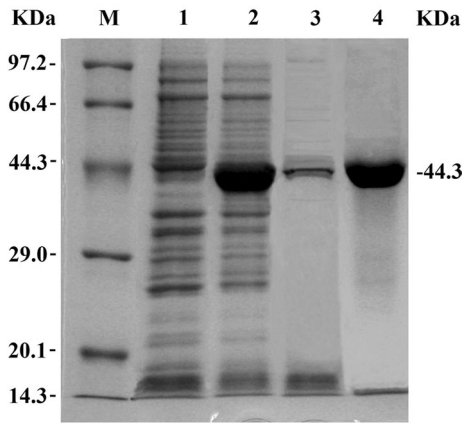

Fig. 2 SDS-PAGE analysis of the expressed re-AuEH2. *Lane M*, protein marker; *lane 1*, the cell lysate of a negative control (*E. coli* BLC); *lane 2*, the soluble portion of *E. coli*/pET-28a-*Aueh2* cell lysate; *lane 3*, the debris of *E. coli*/pET-28a-*Aueh2* cell lysate; *lane 4*, the purified re-AuEH2 with an apparent molecular weight of 44.3 kDa expressed by *E. coli*/pET-28a-*Aueh2*

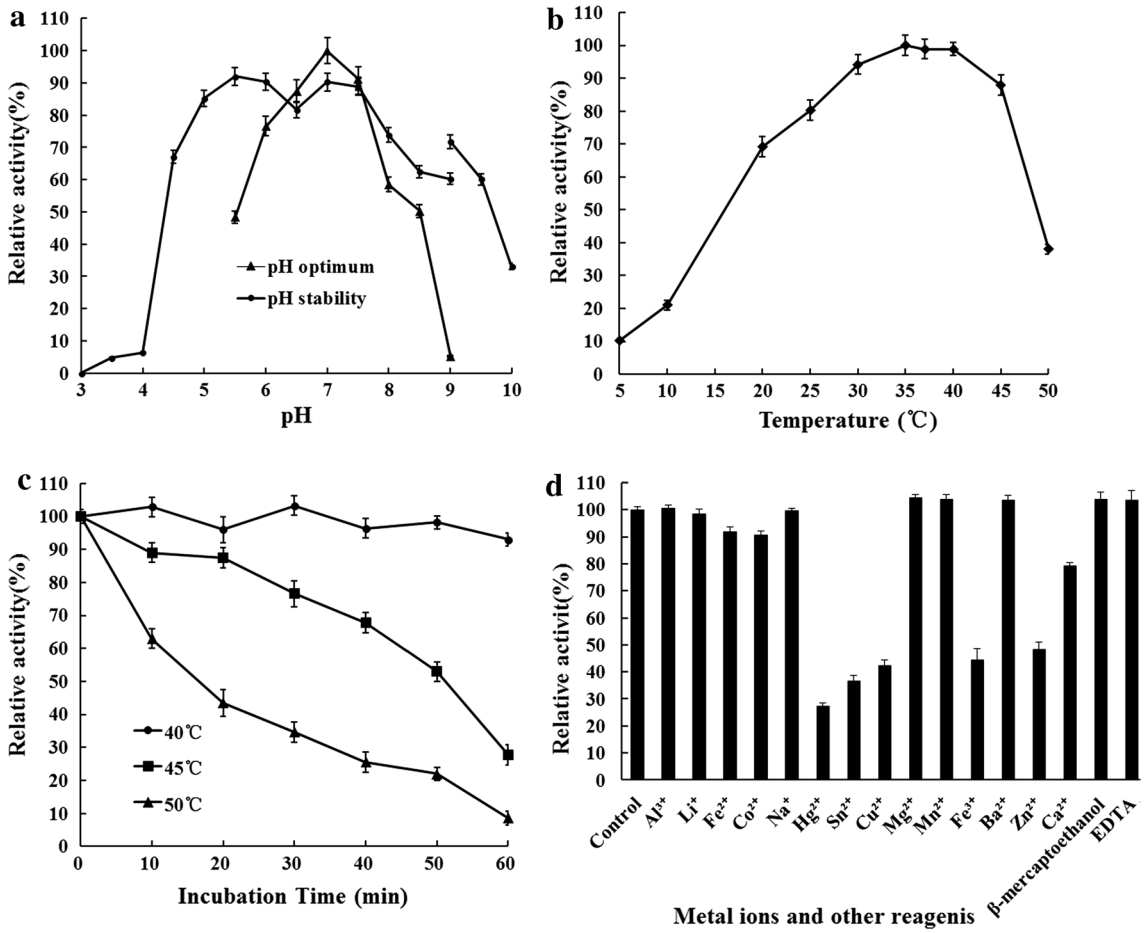

Fig. 3 The enzymatic properties of purified re-AuEH2. **a** Effects of pH values on the catalytic activity and stability of re-AuEH2. **b** Effects of temperatures on the catalytic activity of re-AuEH2. **c** Effects of temperatures on the thermostability of re-AuEH2. **d** Effects of β-mercaptoethanol, EDTA and an array of metal ions on the activity of re-AuEH2

Table 1 The kinetic parameters of purified re-AuEH2 towards (*R*)-SO and (*S*)-SO

Substrate	K_m (mM)	V_{max} (U/mg)	k_{cat} (s^{-1})	k_{cat}/K_m (mM^{-1} s^{-1})
(*R*)-SO	5.90 ± 0.64	20.10 ± 2.33	15.5 ± 1.72	2.77 ± 0.56
(*S*)-SO	7.66 ± 0.51	3.19 ± 0.36	2.36 ± 0.27	0.31 ± 0.05

α/β hydrolase fold enzymes [5]: a nucleophile motif of GGDIGS (identical to Sm-X-Nu-X-Sm–Sm, Sm: small residue, Nu: nucleophile residue, and X: any residue), a motif of HGWP, and an octapeptide of GGHFAALE (Fig. 1). The nucleophile Asp and general-base His of EH catalytic triad are absolutely conserved, while another charge-relay residue is Glu or Asp [9, 22]. Therefore, the catalytic triad of AuEH2 was predicted to be Asp191-His369-Glu343. In addition, two residues, Tyr249 and Tyr312, of AuEH2 are also conserved, which are implicated in substrate binding and oxirane ring opening via hydrogen bonds [15, 25]. It was verified that most of fungal EHs belonged to the microsomal EH family, which showed the low identity at the membrane anchor of 'N-terminal meander' (residues 1-82) [16].

Expression and purification of re-AuEH2

After *E. coli*/pET-28a-*Aueh2* was induced at 28 °C for 8 h, the activity of re-AuEH2 reached 1.44 U/ml, but no EH activity was detected in *E. coli* BLC under the same expression conditions. Rather low re-AuEH2 activity was detected (date not shown) when the induced temperature exceeded 30 °C, speculating that most of re-AuEH2 molecules were transformed into insoluble inclusion bodies at the elevated temperature. SDS-PAGE analysis displayed that re-AuEH2 fused with a His-tag at the N-terminus was expressed as a soluble form in recombinant *E. coli* cells (Fig. 2, lanes 2 and 3). The apparent molecular weight of

re-AuEH2 was 44.3 kDa, which was close to the theoretical one (44.6 kDa) of AuEH2.

The expressed re-AuEH2 was purified to homogeneity by Ni–NTA column (Fig. 2, lane 4). The purification fold was 2.4 with a yield of 65.7 %. The amount of expressed re-AuEH2 was estimated to account for 41 % of the total amount of *E. coli* protein assayed by BandScan 5.0 software based on the standard marker proteins on SDS-PAGE. The specific activity of purified re-AuEH2 was 9.7 U/mg, much higher than those of other well-known EHs from *A. niger* M200 (0.64 U/mg) [8], *Agrobacterium radiobacter* AD1 (1.04 U/mg) [16] and *Solanum tuberosum* (2.0 U/mg) [14].

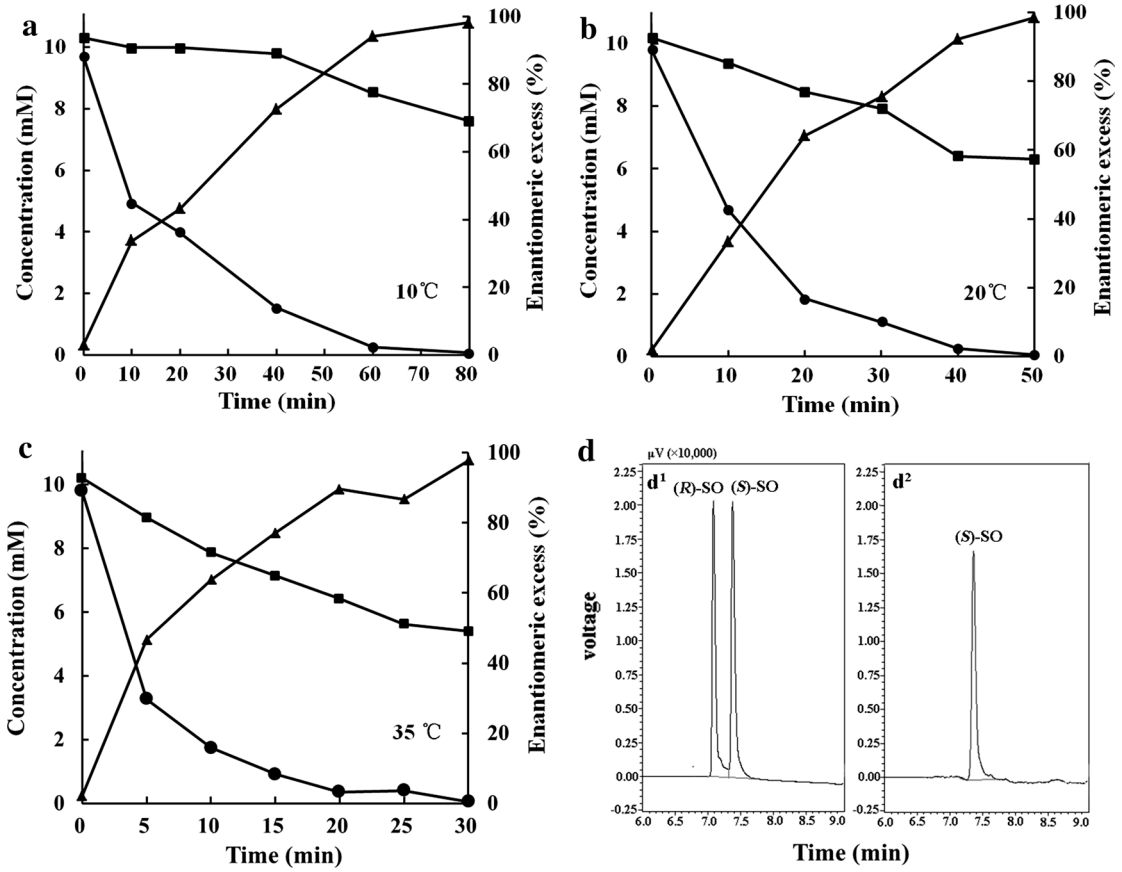

Fig. 4 Resolution of 20 mM racemic SO by re-AuEH2 at 10 °C for 80 min (**a**), 20 °C for 50 min (**b**), and 35 °C for 30 min (**c**). Symbols: *filled circle*, (*R*)-SO; *filled square*, (*S*)-SO; *filled triangle*, enantiomeric excess (ee). **d** GC analysis of the resolution of racemic SO by re-AuEH2 with a chiral CP-Chirasil-DEX CB column and a flame ionization detector. d^1 substrate (*R*,*S*)-SO and d^2 product (*S*)-SO with a 99.2 % ee

Table 2 The resolution of racemic SO by several EHs for the preparation of (*S*)-SO

Enzyme source	Catalytic form	Conc. (mM)	Temp. (°C)	Time (min)	(*S*)-SO ee (%)	Yield (%)	E^a	Reference
A. usamii E001	Enzyme	20	10	80	99.2	38	24.2	This study
A. niger M200	Enzyme	10	20	NI[c]	99	NI	9	[8]
A. niger LCP521	Cells	8	27	120	99	28	10	[1]
R. glutinis	*P. pastoris* cells	4	35	960	>98	36	8–16	[11]
A. radiobacter AD1	Enzyme	5	30	48	99	33	16.2	[19]
Sphingomonas sp. HXN-200[b]	*E. coli* cells	200	30	150	99.1	41.6	30	[23]

[a] Enantiomeric ratio (*E*) was calculated with an equation: $E = [\ln (R_0/R)]/[\ln (S_0/S)]$

[b] The resolution of racemic SO by SpEH was performed in a biphasic system consisting of *n*-hexane/aqueous buffer (1:1)

[c] No information

Enzymatic properties of the purified re-AuEH2

The purified re-AuEH2 exhibited higher activity at pH 6.5–7.5, over which the highest EH activity was at pH 7.0 (measured at 35 °C). It was stable at a pH range of 5.0–7.5, retaining more than 85 % of its original activity (Fig. 3a), which was similar to that of *A. niger* EH [7]. The temperature optimum of re-AuEH2, measured at pH 7.0, was 35 °C (Fig. 3b). The purified re-AuEH2 was highly thermostable at 40 °C until 1 h, retaining over 90 % of its original activity, which was much higher than that (50 %) of *A. niger* EH [7]. Its half-lives ($t_{1/2}$) at 45 and 50 °C were 50 and 15 min (Fig. 3c), respectively.

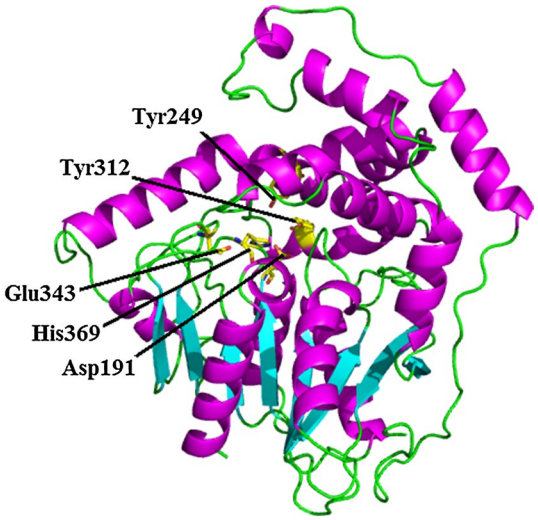

Fig. 5 The 3-D structure of AuEH2 homologically modeled using the MODELLER 9.9 program based on the known crystal structure of *A. niger* EH (AnEH, PDB 1QO7). The modeled 3-D structure consists mainly of an α/β domain containing a catalytic triad Asp191-His369-Glu343, a lid having two active site residues Tyr249 and Tyr312, and an 'N-terminal meander'

The re-AuEH2 activity was not significantly affected by β-mercaptoethanol, EDTA, Al^{3+}, Na^{+}, Li^{+}, Mg^{2+}, Mn^{2+} and Ba^{2+}, but strongly inhibited by Hg^{2+}, Sn^{2+}, Cu^{2+}, Fe^{3+} and Zn^{2+} with only 27.3–48.2 % of its original activity (Fig. 3d). The K_m and V_{max} of re-AuEH2 towards (*R*)-SO were 5.90 mM and 20.1 U/mg, respectively, while towards (*S*)-SO 7.66 mM and 3.19 U/mg. In addition, the k_{cat}^{R} of 15.5 s^{-1} was 6.6-fold higher than k_{cat}^{S} of 2.36 s^{-1} (Table 1). The ratio calculated from $(k_{cat}^{R}/K_{m}^{R})/(k_{cat}^{S}/K_{m}^{S})$ was 8.9, which represented the degree of preferential hydrolysis of one enantiomer over the other at the low concentration [6]. These results showed that re-AuEH2 has high enantioselectivity towards racemic SO, preferentially converting (*R*)-SO, while retaining (*S*)-SO.

Resolution of racemic SO by re-AuEH2

(*S*)-SO with high purity (ee > 99 %) was obtained from resolution of racemic SO by re-AuEH2 (Fig. 4). The yield of (*S*)-SO and *E* value of re-AuEH2 was 38 % (theoretical yield 50 %) and 24.2, respectively, after asymmetrically hydrolysis at 10 °C for 80 min (Fig. 4a), 32 % and 12.2 at 20 °C for 50 min (Fig. 4b), and 27.5 % and 10.3 at 35 °C for 30 min (Fig. 4c). As the temperature increased from 10 to 35 °C, the hydrolysis rate increased, but the yield (38–27.5 %) and *E* value (24.2–10.3) decreased. As listed in Table 2, the enantioselectivity (*E* value) of re-AuEH2 for the preparation of (*S*)-SO was higher than those of other EHs except for SpEH from *Sphingomonas* sp. HXN-200 [23].

MD simulation between AuEH2 and (*R*)-SO or (*S*)-SO

Based on the crystal structure of AnEH (PDB code: 1QO7), sharing 59.0 % primary structure identity with AuEH2, the 3-D structure of AuEH2 was homologically modeled

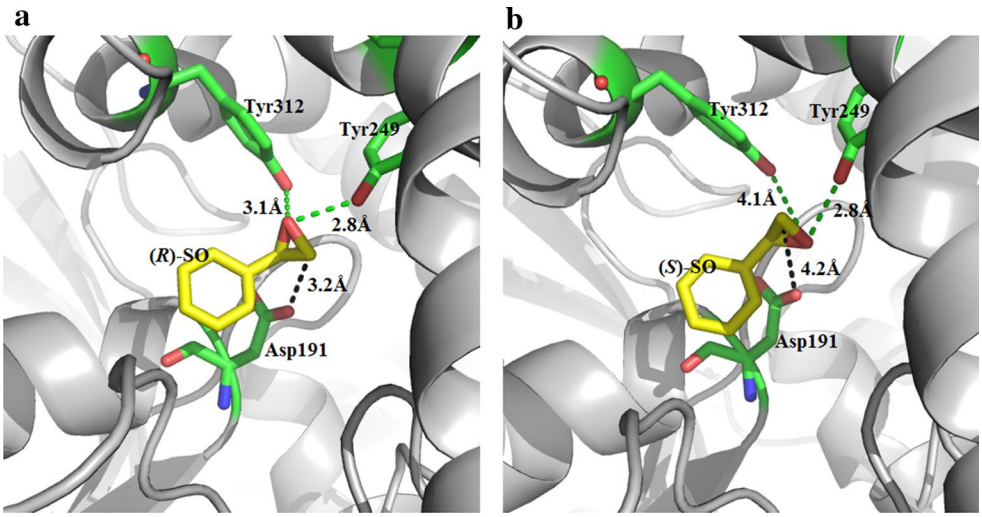

Fig. 6 The molecule-docked conformation of AuEH2 with (*R*)-SO (**a**) or (*S*)-SO (**b**). Asp191, Tyr249 and Tyr312 in the binding pocket of AuEH2 were indicated by *green sticks*, while (*R*)-SO and (*S*)-SO by *yellow sticks*. The hydrogen bond between hydroxyl group of Tyr249 or Tyr312 and O-atom of (*R*)-SO or (*S*)-SO ring was shown by *green dashed line*. The distance between O-atom of nucleophile Asp191 and unsubstituted C-atom of (*R*)-SO or (*S*)-SO ring was indicated by *black dashed line* (color figure online)

(Fig. 5). The AuEH2 3-D structure can be divided into three parts: a core α/β domain that contains a catalytic triad, a lid (residues 230–316) protruding from the α/β domain, and an 'N-terminal meander' (residues 1–82) that in turn caps the lid. The α/β domain follows the classic design of an α/β hydrolase family [28], consisting of a twisted eight-stranded β-sheet sandwiched by six α-helices on both faces. The catalytic triad Asp191-His369-Glu343 and two active site residues Tyr249 and Tyr312 are located in the center of AuEH.

To analyze the enantioselective mechanism of AuEH2 biasing towards (*R*)-SO, MD simulation was performed by AutoDock 4.2. As a result, (*R*)-SO or (*S*)-SO was automatically docked into the binding pocket of AuEH2 (Fig. 6) with similar ΔG_{bind} values, −26.96 and −25.69 kcal/mol. The mechanistic and structural study on AnEH demonstrated that two requirements, activation by hydrogen bonds from two Tyr residues and an optimal positioning of epoxide so that the distance between O-atom of Asp192 and C-atom of epoxide ring is in the range of 3.5–4.0 Å, need to be fulfilled for a smooth reaction [17, 18]. In this work, both Tyr249 and Tyr312 of AuEH2 can form hydrogen bonds with O-atom of epoxide. The hydrogen bond length of Tyr312 with (*R*)-SO (3.1 Å) is shorter than that of Tyr312 with (*S*)-SO (4.1 Å). The distance from O-atom of Asp191 to unsubstituted C-atom of (*R*)-SO was 3.2 Å, while to unsubstituted C-atom of (*S*)-SO 4.2 Å, indicating that (*R*)-SO is the near attack conformation. As discussed by Bruice, the catalytic efficacy of enzyme is dependent on how often the nucleophile and electrophile are present in near attack conformation [2]. Those analytical results suggested that AuEH2 biases towards (*R*)-SO, which are consistent with the experimental results of kinetic parameters and resolution of racemic SO.

Conclusions

In this work, both the full-length cDNA and complete DNA sequences of a novel gene *Aueh2* were amplified from *A. usamii* E001 by different PCR techniques. The nucleotide sequence of *Aueh2* and its deduced amino acid sequence of AuEH2 were analyzed, respectively. Subsequently, an AuEH2-encoding cDNA fragment (ORF) was heterologously expressed in *E. coli* BL21(DE3). The expressed re-AuEH2 displayed the high specific activity, lower K_m and higher V_{max} values towards (*R*)-SO, wider range of pH stability, and strong resistance to β-mercaptoethanol, EDTA and most of metal ions tested. In addition, the resolution of racemic SO by re-AuEH2 to obtain (*S*)-SO was conducted with high ee and yield. All these superior enzymatic properties will make re-AuEH2 a promising candidate for the preparation of optically active epoxides and vicinal diols. Furthermore, the 3-D structures of AuEH2, (*R*)-SO and (*S*)-SO were homologically modeled, respectively, and the enantioselective mechanism of re-AuEH2 biasing towards (*R*)-SO was analyzed by MD simulation.

Acknowledgments This work was financially supported by the National Nature Science Foundation of China (No. 31271811), the Fundamental Research Funds for the Central Universities of China (JUSRP51412B), and the Postgraduate Innovation Training Project of Jiangsu, China (No. CXZZ13_0757). We are grateful to Prof. Xianzhang Wu (School of Biotechnology, Jiangnan University, China) for providing technical assistance.

References

1. Arand M, Hemmer H, Durk H, Baratti J, Archelas A, Furstoss R, Oesch F (1999) Cloning and molecular characterization of a soluble epoxide hydrolase from *Aspergillus niger* that is related to mammalian microsomal epoxide hydrolase. Biochem J 344:273–280
2. Bruice TC (2002) A view at the millennium: the efficiency of enzymatic catalysis. Acc Chem Res 35:139–148
3. Chen CS, Fujimoto Y, Girdaukas G, Sih CJ (1982) Quantitative analyses of biochemical kinetic resolutions of enantiomers. J Am Chem Soc 104:7294–7299
4. Choi WJ (2009) Biotechnological production of enantiopure epoxides by enzymatic kinetic resolution. Appl Microbiol Biotechnol 84:239–247
5. Holmquist M (2000) Alpha/Beta-hydrolase fold enzymes: structures, functions and mechanisms. Curr Protein Pept Sci 1:209–235
6. Kim HS, Lee SJ, Lee EJ, Hwang JW, Park S, Kim SJ, Lee EY (2005) Cloning and characterization of a fish microsomal epoxide hydrolase of *Danio rerio* and application to kinetic resolution of racemic styrene oxide. J Mol Catal B Enzym 37:30–35
7. Kotik M, Kyslík P (2006) Purification and characterisation of a novel enantioselective epoxide hydrolase from *Aspergillus niger* M200. Biochim Biophys Acta 1760:245–252
8. Kotik M, Štěpánek V, Kyslík P, Marešová H (2007) Cloning of an epoxide hydrolase-encoding gene from *Aspergillus niger* M200, overexpression in *E. coli*, and modification of activity and enantioselectivity of the enzyme by protein engineering. J Biotechnol 132:8–15
9. Labuschagne M, Albertyn J (2007) Cloning of an epoxide hydrolase-encoding gene from *Rhodotorula mucitaginosa* and functional expression in *Yarrowia lipolytica*. Yeast 24:69–78
10. Laemmli UK (1970) Cleavage of structural proteins during the assembly of the head of bacteriophage T4. Nature 227:680–685
11. Lee EY, Yoo SS, Kim HS, Lee SJ, Oh YK, Park S (2004) Production of (*S*)-styrene oxide by recombinant *Pichia pastoris* containing epoxide hydrolase from *Rhodotorula glutinis*. Enzyme Microb Technol 35:24–631
12. Liu ZQ, Zhang LP, Cheng F, Ruan LT, Hu ZC, Zheng YG, Shen YC (2011) Characterization of a newly synthesized epoxide hydrolase and its application in racemic resolution of (R, S)-epichlorohydrin. Catal Commun 16:133–139
13. Li JF, Wei XH, Tang CD, Wang JQ, Zhao MH, Pang QF, Wu MC (2014) Directed modification of the *Aspergillus usamii* β-mannanase to improve its substrate affinity by in silico design and site-directed mutagenesis. J Ind Microbiol Biotechnol 41:693–700
14. Monterde MI, Lombard M, Archelas A, Cronin A, Arand M, Furstoss R (2004) Enzymatic transformations. Part 58: enantioconvergent biohydrolysis of styrene oxide derivatives catalysed

by the *Solanum tuberosum* epoxide hydrolase. Tetrahedron Asymmetry 15:2801–2805
15. Rink R, Kingma J, Lutje Spelberg JH, Janssen DB (2000) Tyrosine residues serve as proton donor in the catalytic mechanism of epoxide hydrolase from *Agrobacterium radiobacte*r. Biochemistry 39:5600–5613
16. Rui L, Cao L, Chen W, Reardon KF, Wood TK (2005) Protein engineering of epoxide hydrolase from *Agrobacterium radiobacter* AD1 for enhanced activity and enantioselective production of (*R*)-1-phenylethane-1,2-diol. Appl Environ Microbiol 71:3995–4003
17. Reetz MT, Bocola M, Wang LW, Sanchis J, Cronin A, Arand M, Zou JY, Archelas A, Bottalla AL, Naworyta A, Mowbray SL (2009) Directed evolution of an enantioselective epoxide hydrolase: uncovering the source of enantioselectivity at each evolutionary stage. J Am Chem Soc 131:7334–7343
18. Reetz MT (2012) Laboratory evolution of stereoselective enzymes as a means to expand the toolbox of organic chemists. Tetrahedron 68:7530–7548
19. Lutje Spelberg JH, Rink R, Kellogg RM, Janssen DB (1998) Enantioselectivity of a recombinant epoxide hydrolase from *Agrobacterium radiobacter*. Tetrahedron: Asymmetry 9:459–466
20. Wang ZQ, Wang YS, Su ZG (2013) Purification and characterization of a *cis*-epoxysuccinic acid hydrolase from *Nocardia tartaricans* CAS-52, and expression in *Escherichia coli*. Appl Microbiol Biotechnol 97:2433–2441
21. Weijers CAGM, de Bont JAM (1999) Epoxide hydrolases from yeasts and other sources: versatile tools in biocatalysis. J Mol Catal B Enzym 6:199–214
22. Woo JH, Kang JH, Kang SG, Hwang YO, Kim SJ (2009) Cloning and characterization of an epoxide hydrolase from *Novosphingobium aromaticivorans*. Appl Microbiol Biotechnol 82:873–881
23. Wu S, Li A, Chin YS, Li Z (2013) Enantioselective hydrolysis of racemic and *meso*-epoxides with recombinant *Escherichia coli* expressing epoxide hydrolase from *Sphingomonas* sp. HXN-200: preparation of epoxides and vicinal diols in high ee and high concentration. ACS Catal 3:752–759
24. Wu MC, Wang JQ, Zhang HM, Tang CD, Gao JH, Tan ZB (2011) Cloning and sequence analysis of an acidophilic xylanase (XynI) gene from *Aspergillus usamii* E001. World J Microbiol Biotechnol 27:831–839
25. Yamada T, Morisseau C, Maxwell JE, Argiriadi MA, Christianson DW, Hammock BD (2000) Biochemical evidence for the involvement of tyrosine in epoxide activation during the catalytic cycle of epoxide hydrolase. J Biol Chem 275:23082–23088
26. Yildirim D, Tukel SS, Alagoz D, Alptekin O (2011) Preparative-scale kinetic resolution of racemic styrene oxide by immobilized epoxide hydrolase. Enzym Microb Technol 49:555–559
27. Zhou CY, Bai HY, Deng SS, Wang J, Zhu J, Wu MC, Wang W (2008) Cloning of a xylanase gene from *Aspergillus usamii* and its expression in *Escherichia coli*. Bioresour Technol 99:831–838
28. Zou J, Hallberg BM, Bergfors T, Oesch F, Arand M, Mowbray SL, Jones TA (2000) Structure of *Aspergillus niger* epoxide hydrolase at 1.8 Å resolution: implications for the structure and function of the mammalian microsomal class of epoxide hydrolases. Structure 8:111–122